Supporting information

Jian Feng [a, b], Dongxia Yan [b, c, e] *, Chunrui Rong [b, d], Lingzhi Yu [a, b], Jiabao Li [b], Jiayu Xin [b, c], Xingmei Lu [b, c], Qing Zhou [b, c], Ziqing Wang [a, *], Zhong Wei [a, *]

[a] *State Key Laboratory for Green Process of Chemical Engineering of Xinjiang Bingtuan, School of Chemistry and Chemical Engineering, Shihezi University, Shihezi 832003, China*

[b] *Beijing Key Laboratory of Ionic Liquids Clean Process, CAS Key Laboratory of Green Process and Engineering, State Key Laboratory of Mesoscience and Engineering, Institute of Process Engineering, Chinese Academy of Sciences, Beijing 100190, China*

[c] *School of Chemical and Engineering, University of Chinese Academy of Sciences, Beijing 100049, China*

[d] *Sino Danish College, University of Chinese Academy of Sciences, Beijing 100049, China*

[e] *Langfang Technological Centre of Green Industry, Langfang 065006, Hebei, P. R. China*

*Corresponding authors

E-mail: dxyan@ipe.ac.cn (Dongxia Yan), wzq20070420@163.com (Ziqing Wang), steven_weiz@sina.com (Zhong Wei)

Scale-up synthesis of PA4F

We carried out the prepolymerization reaction in the reactor according to the preferred conditions, and put 0.3 mol DMFDC, 100 ml H_2O, 1.1 wt% [Bmim][H_2PO_4], and 0.309 mol BDA into the reactor in turn. During the polycondensation stage, we utilized a 250 ml three-port round-bottomed flask equipped with a condenser and vacuum trap, and an overhead stirrer. The air in the reactor was replaced with argon three times, and the pressure was charged to 0.4 MPa. The reaction was carried out at 80°C for 1 h, then increased to set temperature 150°C and maintained for 3 h. In the polymerization step performed under argon, transfer the aqueous solution of the prepolymer into a flask, and the mechanical

stirring speed was adjusted to 60 rpm, then it was heated at 80°C for 1 h by monitoring the temperature of the oil bath, to remove the methanol produced by the amine transesterification reaction. The mixture was then dehydrated under reduced pressure at 130°C for 0.5 h, resulting in the formation of white solid agglomerates due to the removal of water. The stirrer stopped rotating due to excessive torque. The temperature was increased to 160°C and the vacuum was maintained at 100 Pa for 0.5 h. The temperature was then raised to 190°C, and the system was melted. Mechanical stirring was initiated and the speed was adjusted with the torque. Vacuum polycondensation was performed for 2 h. The temperature was then raised to 230°C. After stirring for 1.2 h in the molten state, the stirrer overloaded and stopped rotating. To maintain consistency with the desired conditions, the polycondensation time was kept at 6 h, and argon was used to cool the mixture to room temperature. Due to the hardening of the polymer on the bottle wall, heat transfer and the escape of small molecules are limited. Therefore, we randomly sampled near the bottle wall by GPC for analysis. The obtained polymer M_n = 23.0 kg/mol, M_w = 39.3 kg/mol, PDI=1.71.

Fig. S1 The picture of scale-up synthesized PA4F

Spectroscopic Characterization

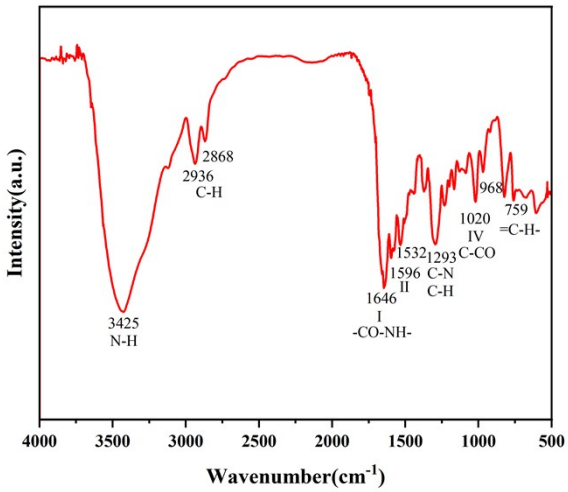

Fig. S2 FT-IR of PA4F[1].

The peak at 3425 cm^{-1} is the N-H stretching vibration absorption peak; the peaks at 2936 cm^{-1} and 2868 cm^{-1} are the asymmetric and symmetric C-H stretching vibration peaks; the peak at 1646 cm^{-1} is the stretching vibration absorption peak of the amide bond (amide I band); the peaks at 1532 cm^{-1} and 1596 cm^{-1} were the combined absorption peaks of N-H in-plane bending and C-N stretching vibration (amide II band); the peak at 1293 cm^{-1} was the combined absorption peak of C-N stretching vibration and C-H in-plane bending (amide III band); and the peak at 1020 cm^{-1} was the absorption peak of C=O stretching vibration (amide IV band); the appearance of these peaks proved that the amide bond was present in the product, and meanwhile, the vibration peaks of the furan ring appeared at the positions of 1020 cm^{-1}, 968 cm^{-1} and 759 cm^{-1}.

NMR analysis of PA4F

(^{1}H NMR, 700 MHz, DMSO-d6, δ ppm, 298 K): 8.48 (2H, -N**H**-CO-furan-CO-NH-), 7.10 (2H, =C**H**- of furan ring), 3.29 (4H, -NH-C**H**$_2$-(CH$_2$)$_2$-C**H**$_2$-NH-), 1.55 (4H, -NH-CH$_2$-(C**H**$_2$)$_2$-CH$_2$-NH-).

(^{13}C NMR, 700 MHz, DMSO-d6, δ ppm, 298 K): 157.15 (2C, -NH-**C**O-furan-**C**O-NH-) 148.14 (2C, O-**C**H- of furan ring), 114.27 (2C, =**C**H- of furan ring), 26.85 (2C, -NH-**C**H$_2$-(CH$_2$)$_2$-**C**H$_2$-NH-), 38.19 (2C, -NH-CH$_2$-(**C**H$_2$)$_2$-CH$_2$-NH-).

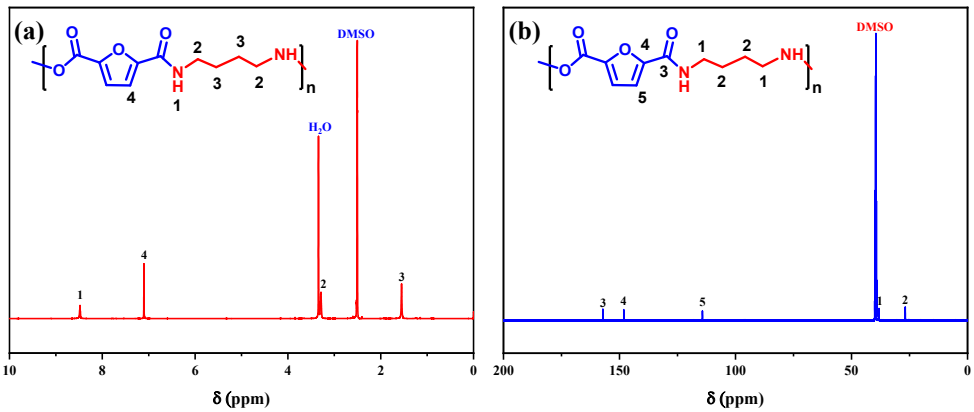

Fig. S3 (a)^{1}H NMR and (b) ^{13}C NMR spectrum of PA4F[1].

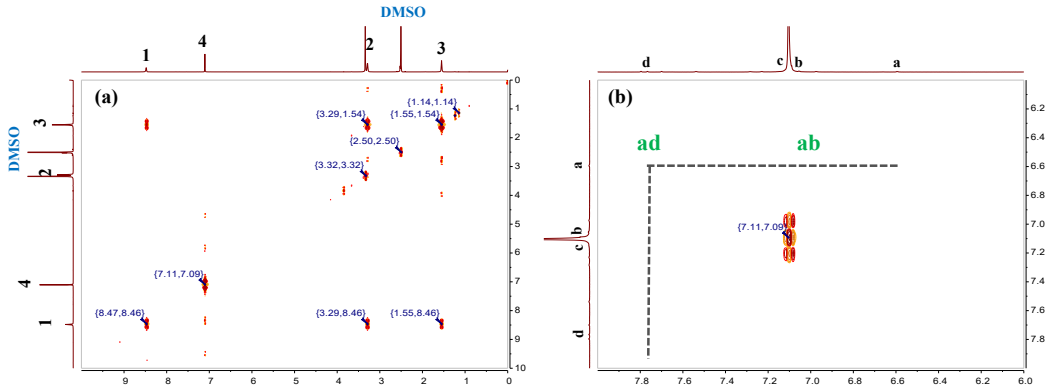

Fig. S4 2D TOCSY of PA4F[1] (DMSO-d6) (a) range 0.5-9.5 ppm. (b) range 6-8.0 ppm.

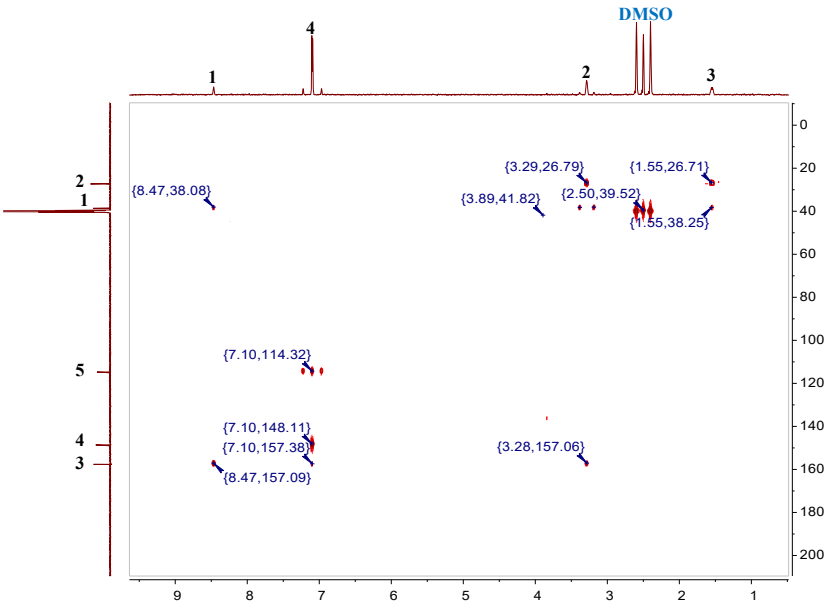

Fig. S5 2D HMBC of PA4F[1] (DMSO-d6).

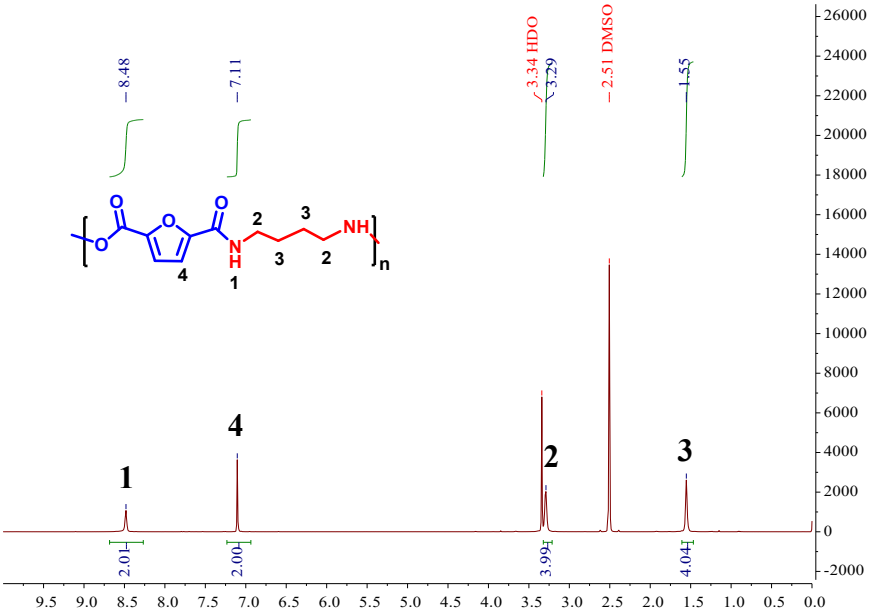

Fig. S6 [1]H NMR spectrum recorded for PA4F[1] polymer in DMSO-d6.

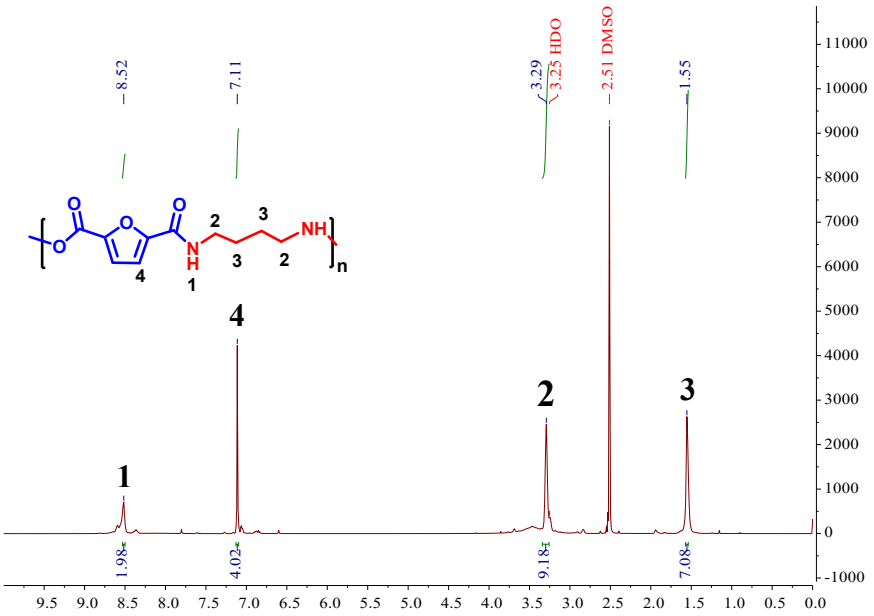

Fig. S7 ^{1}H NMR spectrum recorded for PA4F^{2} polymer in DMSO-d6.

Table S1. HMBC data of PA4F^{1}.

Group	HMBC atoms			
	Hydrogen		Carbon	
	Code	Chemical shift (ppm)	Code	Chemical shift (ppm)
			5	114.32
H H	4	7.10	4	148.11
			3	157.38
			1	38.08
H	1	8.47	3	157.09

Table S2. Comparison of diamine unit to diester moiety ratio in feed and polymer.

Run	Feed ratio	-NH-F-NH in polymer	-CH_2-CH_2 in polymer
	Diamine/diester	n_F	n_B
PA4F[1]	1.05	1.00	1.01
PA4F[2]	1.05	0.49	0.77

Due to the stability of the hydrogen on the furan ring (H-4) and the CH_2 (H-2) linked to the amide bond in BDA chains, they are selected for quantitative analysis. Here, n_F represents the percentage of the furan ring involved in the formation of -NH-F-NH- in the polymer chains, and n_B represents the deviation percentage of adjacent CH_2 in BDA segments in different chemical environments. Both values are expected to be close to 1 in polymer chains. n_B and n_F can be calculated with the following formula:

$$n_F = {}^{I_{H1}}/_{I_{H4}}, n_B = {}^{I_{H3}}/_{I_{H2}}$$

Where I_{H3} is the integral corresponding to the CH_2 protons (H-3), I_{H2} is the integral of CH_2 (H-2) linked to the amide bond in BDA chains, I_{H4} is the integral corresponding to the hydrogen on the furan ring (H-4), I_{H1} is the integral corresponding to the hydrogen in the amide (H-1).

ESI-MS spectrometry analysis

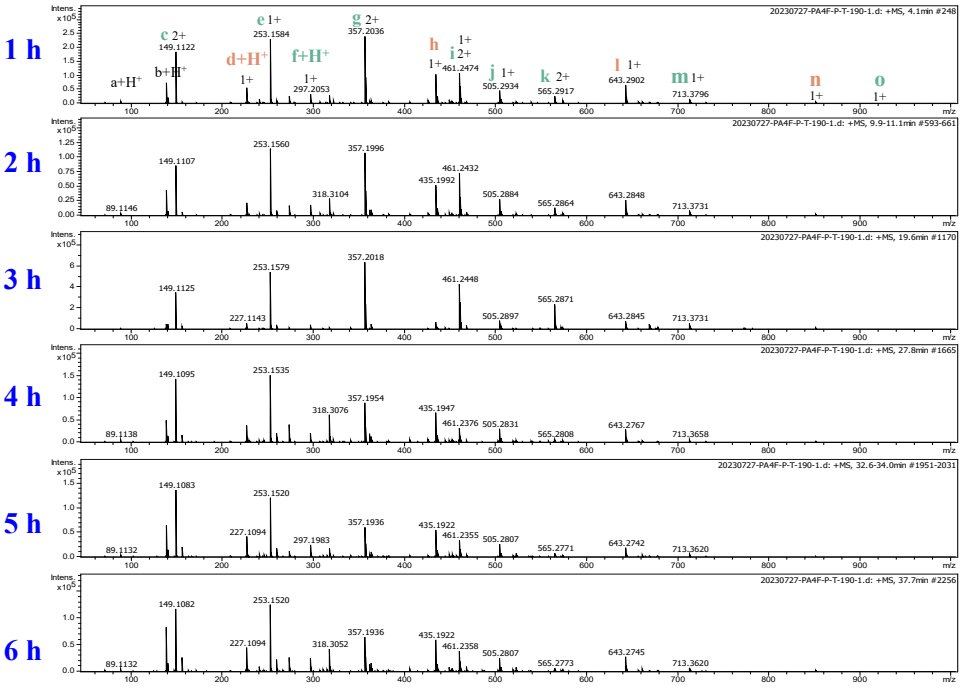

Fig. S8 ESI-MS spectra of samples at different times under 190°C.

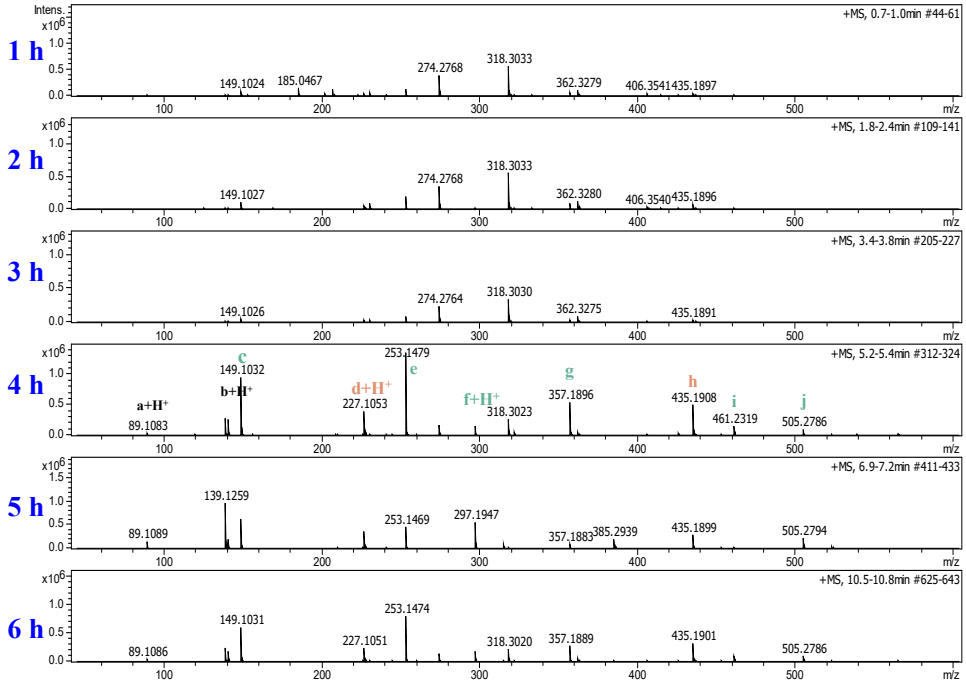

Fig. S9 ESI-MS spectra of samples at different times under 150°C.

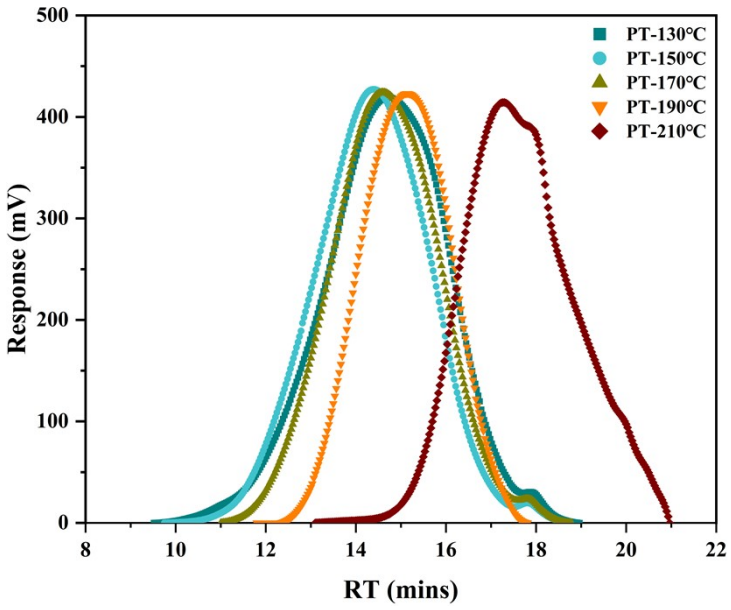

Fig. S10 GPC curves of PA4F at different prepolymerization temperature.

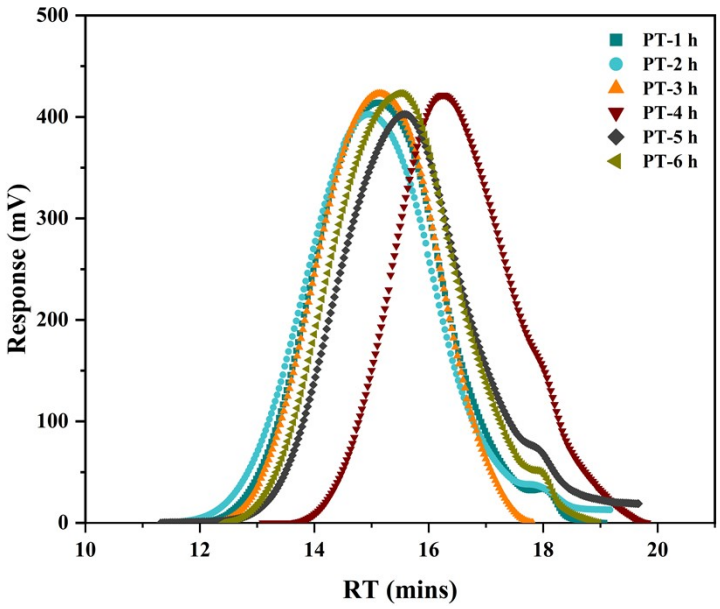

Fig. S11 GPC curves of PA4F at different prepolymerization time

MALDI-TOF MS spectrometry analysis

The chemical structure of PA4F is further characterized in this section, with a focus on the end groups. Different series of end groups, deviating from the expected amino and ester groups, were identified. The peak intensity of these end groups was compared by m-Mass spectrometry and sorted to Table S3.

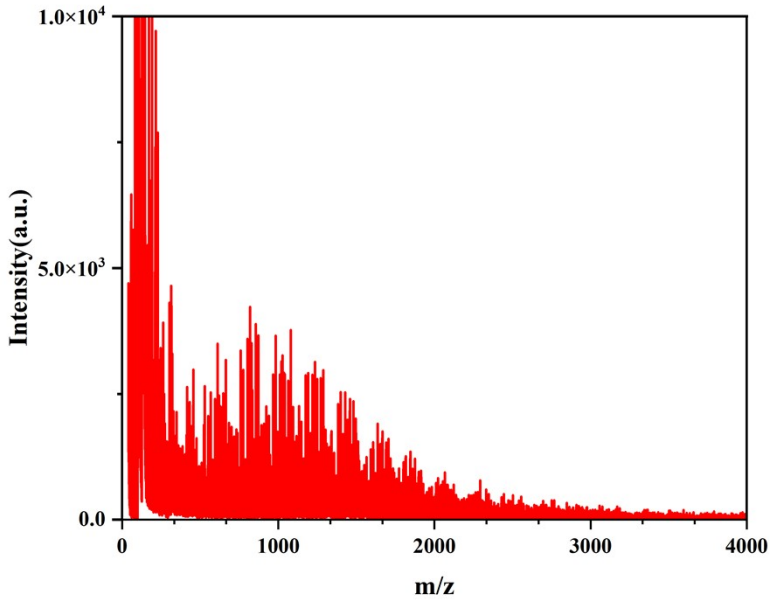

Fig. S12 MALDI-TOF MS spectrum of PA4F[2].

Table S3. MALDI-TOF MS end-group assignments for PA4F.

Series	Proposed end-groups	M_{EG} (cation)Assign.	M_{EG} (ins) Obs[1].	M_{EG} (ins) Obs[2].
1	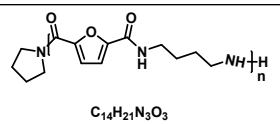 $C_{14}H_{21}N_3O_3$ 279.16	1111.49 (H^+)	1111.41 (1183)	1111.41 (552)
2	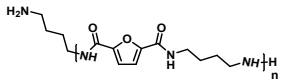 $C_{14}H_{24}N_4O_3$ 296.18	1151.51 (Na^+)	1151.48 (644)	1148.45 (1143)
3	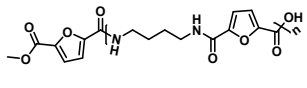 $C_{17}H_{18}N_2O_8$ 378.11	1233.43 (Na^+)	1231.51 (619)	1233.52 (1953)
4	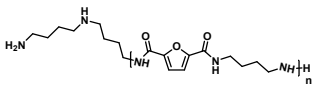 $C_{18}H_{33}N_5O_3$ 367.26	1222.58 (Na^+)	1222.35 (503)	1219.50 (2899)
5	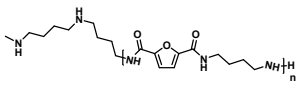 $C_{19}H_{35}N_5O_3$ 381.27	1236.60 (Na^+)	1236.60 (326)	1235.55 (2480)
6	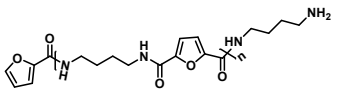 $C_{19}H_{26}N_4O_5$ 390.19	1245.51 (Na^+)	1244.51 (1045)	1244.57 (1470)
7	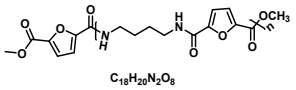 $C_{18}H_{20}N_2O_8$ 392.12	1303.46 (Na^+)	1301.61 (4234)	1301.63 (1178)

The samples labeled Obs[1] are from the samples with a prepolymerization temperature of 150°C during the conditional screening process, and the samples labeled Obs[2] are from the samples with a prepolymerization temperature of 210°C during the conditional screening process.

Table S4. Structures of the main chain segments.

	Structure	N	M	N	M
BH	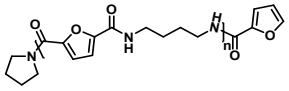	1	373.161	8	1831.040
		2	581.253	9	2039.717
		3	789.259	10	2248.855
		4	997.402	11	2459.130
		5	1205.531	12	2669.875
		6	1413.882	13	2879.126
		7	1622.405	14	3088.115
AH	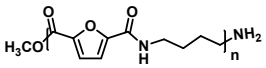	1	469.202	8	1928.300
		2	677.238	9	2137.166
		3	885.265	10	2347.228
		4	1094.205	11	2556.469
		5	1301.395	12	2765.906
		6	1511.050	13	2975.662
		7	1719.549		

AH represents heteropolymer with active end groups, which has a methoxyl group at one end of the polymer chain, with the other end being an amine. BH is heteropolymer with blocked groups, pyrrolidine group at one end and decarboxylated FDCA at the other, these types of chain ends prevent the growth of the chains.

XRD

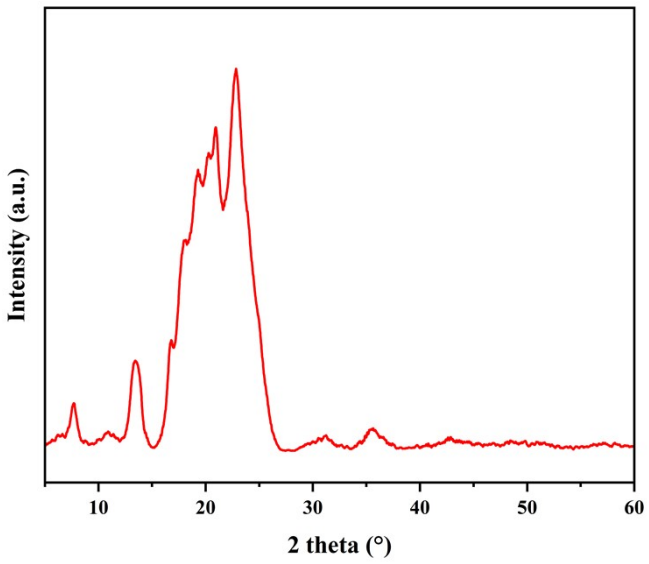

Fig. S13 WAXD spectrum of PA4F[1].

Mechanical property

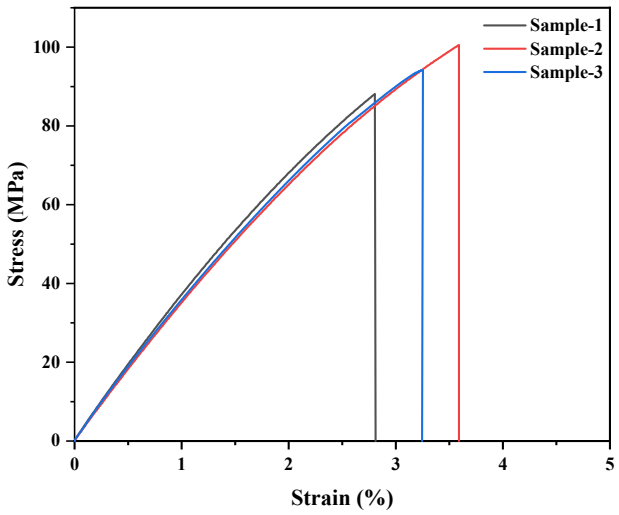

Fig. S14 Stress-strain curves for PA4F compression moulded specimens.

Viscoelastic properties

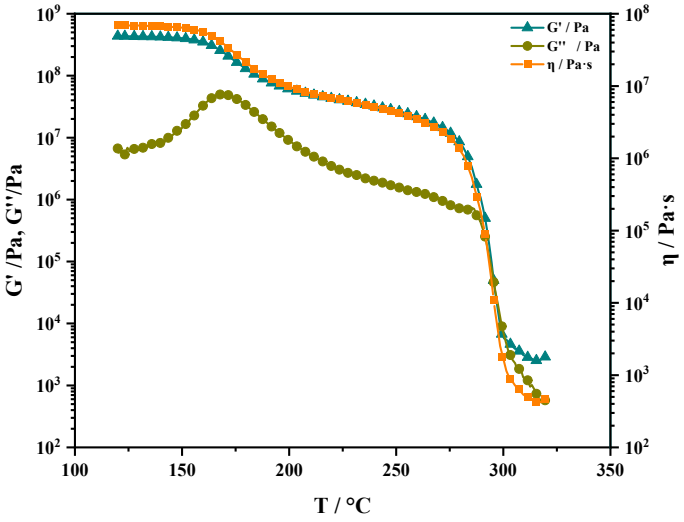

Fig. S15 The temperature dependence of the storage and loss moduli (G' and G'') and complex viscosity (η) for the scale-up synthesis of PA4F product.

Computational details

DFT calculations were performed with Gaussian 16[1] program. All molecular geometries were optimized in gas phase at the B3LYP[2]/6-31G(d)[3] level of theory using SMD model[4] to account for solvation energies in water at 298.15 K and 1 atm with Grimme's D3[5] dispersion correction. Optimized minima were verified by harmonic vibrational analysis that have no imaginary

frequency. To refine calculated energies, single point calculations with larger basis set def2TZVP[6] were then performed based on these optimized structures by using the same B3LYP-D3BJ functional using SMD as the solvation mode in water.

References

[1] Gaussian 16, Revision C.01,M. J. Frisch, G. W. Trucks, H. B. Schlegel, G. E. Scuseria, M. A. Robb, J. R. Cheeseman, G. Scalmani, V. Barone, G. A. Petersson, H. Nakatsuji, X. Li, M. Caricato, A. V. Marenich, J. Bloino, B. G. Janesko, R. Gomperts, B. Mennucci, H. P. Hratchian, J. V. Ortiz, A. F. Izmaylov, J. L. Sonnenberg, D. Williams-Young, F. Ding, F. Lipparini, F. Egidi, J. Goings, B. Peng, A. Petrone, T. Henderson, D. Ranasinghe, V. G. Zakrzewski, J. Gao, N. Rega, G. Zheng, W. Liang, M. Hada, M. Ehara, K. Toyota, R. Fukuda, J. Hasegawa, M. Ishida, T. Nakajima, Y. Honda, O. Kitao, H. Nakai, T. Vreven, K. Throssell, J. A. Montgomery, Jr., J. E. Peralta, F. Ogliaro, M. J. Bearpark, J. J. Heyd, E. N. Brothers, K. N. Kudin, V. N. Staroverov, T. A. Keith, R. Kobayashi, J. Normand, K. Raghavachari, A. P. Rendell, J. C. Burant, S. S. Iyengar, J. Tomasi, M. Cossi, J. M. Millam, M. Klene, C. Adamo, R. Cammi, J. W. Ochterski, R. L. Martin, K. Morokuma, O. Farkas, J. B. Foresman, and D. J. Fox, Gaussian, Inc., Wallingford CT, 2019.

[2] (a) Becke, A. D. J. Chem. Phys. 1993, 98, 5648−5652. (b) Lee, C.; Yang, W.; Parr, R. G.Phys. Rev. B: Condens. Matter Mater. Phys. 1988, 37, 785−789. (c) Vosko, S. H.; Wilk, L.; Nusair, M. Can. J. Phys. 1980, 58, 1200−1211.

[3] (a) Hehre, W. J.; Ditchfield, R.; Pople, J. A. J. Chem. Phys.1972, 56, 2257-2261. (b) Hariharan, P. C.; Pople, J. A. Theor. Chim. Acta 1973, 28, 213-222.

[4] Marenich, A. V.; Cramer, C. J.; Truhlar, D. G. J. Phys. Chem. B 2009, 113 (18), 6378−6396.

[5] Grimme, S.;Antony, J.; Ehrlich, S.; Krieg, H. J. Chem. Phys. 2010, 132, 154104.

[6] Weigend, F.; Ahlrichs, R. Phys. Chem. Chem. Phys. 2005, 7, 3297-3305